



Combined effects of evaporation and cavitation on the performance of a renewable energy powered natural vacuum desalination unit in Bahrain

T. Ayhan^{a,*}, H. Al-Madani^b

^aMechanical Engineering Department, University of Bahrain, Isa Town, Kingdom of Bahrain, email: tayhan@uob.edu.bh

^bVice President's Office, Kingdom University, Isa Town, Kingdom of Bahrain, email: h.almadani@ku.edu.bh

Received 20 April 2014; Accepted 19 May 2015

ABSTRACT

The renewable energy powered natural vacuum desalination unit (NVDU) presents a promising alternative technique for seawater desalination and wastewater treatment, with low energy consumption, simple technology, and resulting clean environment. The problem of the low daily productivity of the NVDU motivated researchers to investigate various means of improving its productivity and thermal efficiency in order to reduce the production cost of freshwater. This study investigates experimentally the performance of the NVDU under the combined effects of evaporation and cavitation on freshwater production rate. The NVDU consists of an inverse U-shaped pipe, with one side acting as the evaporator and the other side as the condenser. The experiments were conducted under three different sets of conditions. The first had ambient conditions on both sides, the second used a water-ring vacuum pump to create a buoyancy effect, and the third was similar to the second set of conditions, but with cooling of the condensation side. The results show that the last case increased the freshwater production rate by approximately 70 times compared to the first case, while in the second case, the production rate was roughly 13 times better than in the first. These results could be attributed to the combined effects of evaporation and cavitation. This attribution is supported by the visualization of bubble motions.

Keywords: Renewable; Natural vacuum; Desalination; Cavitation

1. Introduction

A lack of freshwater is very hazardous to human health, especially in children, and can result in deaths. It was found that 88 developing countries, representing half of the world's population, are affected by scarcity of freshwater, and more than 80% of all diseases and 30% of all deaths result from poor water quality [1]. Most of the Gulf Cooperation Council (GCC) countries depend on water desalination to meet

their freshwater needs, due to the low availability of renewable freshwater. Generally, these countries have similar oil-driven economies; very large reserves of oil and gas have been discovered in the last few decades and oil exports constitute around 90% of their revenues [2]. Conversely, their natural water resources are being depleted rapidly, while demand for freshwater is increasing due to the growth of the population, leading these countries to acquire half of the world's desalination plants. Most of these plants are driven by natural gas, as it is cost-effective, safer than oil, and better environmentally, but they still produce large

*Corresponding author.

amounts of CO₂ and other pollutants. Among the GCC countries, one that suffers markedly from water scarcity is the Kingdom of Bahrain, much of whose freshwater comes from underground aquifers which are being constantly depleted. To ease the demand on these aquifers, a small number of desalination plants have been constructed; the country now has a production capacity of 64 Mm³/year from three main desalination plants [3].

Many studies have been conducted to enhance the performance of thermal or phase change desalination by generating vacuum inside the desalination unit, resulting in lower evaporation temperatures and less energy to evaporate the water, hence increasing the productivity and efficiency of phase change desalination. Bemporad performed a numerical analysis of the hydrodynamic aspects of solar energy distillation [4]. The design consisted of two chambers connected by a pipe, one chamber for evaporation and the other for the fresh or distilled water. A vacuum was generated inside the system and the saline water was pumped by the difference between the atmospheric pressure, pushing the water to a height of 10.33 m, and the vapor pressure at the hot saline water surface. The main driving force was the difference in vapor pressure between the two chambers; the evaporator was kept at considerably higher temperature than the distilled water chamber. Midilli and Ayhan studied a similar natural vacuum distillation (NVD) system which included balance design and a selection of distillation methods. Natural vacuum formation, balancing, and feeding processes are all introduced and discussed in detail [5]. The same researchers conducted an indoor experimental analysis using waste heat to distill seawater [6]; the concept of vacuum evaporation is the same as in the previous researches. The feasibility of such systems in the Arabian Gulf region, specifically in Bahrain, was studied by Al-Madani and Ayhan [7]. The design was a simple inverted U-shape containing the evaporator on one side and the condenser on the other. The system was installed at a height of 10.33 m to benefit from the natural vacuum produced. Another similar study of NVD was carried out by Veeragnaneswar and Nermalakhandan [8]. Their design used solar radiation directly through the use of a glass cover over the evaporator and a cold plate for condensing the vapor. The experiment was mainly concerned with the use of solar power as the main heat source. The unit produced 7.4 kg/m² per d.

Al-Madani and Ayhan performed an illustrative study of the analytical relations underlying the phenomenon and report that according to their calculations and assumptions, the system is thermodynamically

feasible [7]. The freshwater production rate was 0.022 L/h with an evaporation surface area of 0.0490 m². They later studied applications of NVD for hot and cold climatic conditions using waste heat and renewable resources [9].

The theoretical performance of the natural vacuum unit in an inverse U-shaped geometry was then studied by Alezzi and Ayhan [10]. They present a mathematical model and report the results of a 12-h day simulation. A comparison between hot and cold results is discussed. This result is compared with the previous work of Al-Madani and Ayhan [7] and it is reported that the theoretical simulation result was 26.6% higher.

1.1. Boiling and cold evaporation (cavitation)

In order to enhance the performance of the inverse U-shaped natural vacuum desalination unit (NVDU), a buoyancy-driven and cavitating flow domain was created by adjusting the difference between evaporation temperature and seawater supply temperature (causing buoyancy-driven flow). A water-ring vacuum pump was used to remove noncondensable gases. The evaporation rate was enhanced by creating cavitation in the liquid phase of seawater. Two types of vaporization are known [11,12]. The first is the well-known process of vaporization by increasing the temperature (boiling). The second is vaporization under nearly constant temperature due to reduced pressure, as in the case of cavitation. The insight gained from this fundamental investigation may help to understand evaporation phenomena in the NVDU, which have been observed experimentally, and help in the design and optimization of future combined hot and cold evaporation for seawater desalination using an NVDU.

The experimental work included the establishment of the experimental system and the customization of NVD to the climatic conditions of Bahrain. The prototype NVDU experiments were conducted on the roof of the Mechanical Engineering Department building at the University of Bahrain.

In addition to the experimental work, this study briefly explains the theoretical model and discusses the design of the hot and cold boiling process.

2. Theoretical model and proposed process

The principle behind the NVD system is that water in the system at low pressure evaporates at a relatively low temperature. This results in low energy requirements to vaporize it. As the name implies, the vacuum is generated naturally without the need for a

vacuum pump to generate the required operation conditions. Fig. 1 shows a schematic illustration of an inverted U-shaped NVD system. The driving force for the process is the pressure difference between the two chambers, which exists because the saturation pressure of freshwater is slightly higher than that of saline water at a given temperature; otherwise, the vapor could transfer from the freshwater chamber to the saline water chamber [10]. The thermodynamic cycle of the operation process is indicated by the pressure–enthalpy diagram in Fig. 2. In Figs. 1 and 2, points 1 and 2 represent the sub-cooled liquid phase seawater. As solar radiation falls on the evaporation column M, the temperature increases, changing the density of the water. This effect causes the water at the top of the column (point 3) to be at a low pressure, reaching a natural vacuum and causing continuous evaporation of seawater at the top of the column.

The vapor flows from column M to the condensation column N, which is located in a shaded area where there is no solar radiation. Condensation occurs at point 4 as a result of the temperature difference between points 3 and 4. At point 5, all vapor will be

in the saturated liquid phase. The accumulation of liquid water causes an increase of pressure in column N, reaching points 6 and 7 in Fig. 2. This process continues as long as there is a temperature difference between columns M and N.

The principle of operation of the system is very simple. Four electromagnetic valves, A and B at the bottom of each column and C and D at the top of the upper tank, are provided to control the vacuum creation process. Valve C allows freshwater to be supplied, whereas valve D allows air to be released, as shown in Fig. 1. In order to create a natural vacuum, valves A and B are closed, and C and D are opened, until water fills the whole system. This initial phase is done only once at the start-up of the system. Valves C and D are then closed, while valves A and B remain open. The water level drops until it reaches an equilibrium position of 10.33 m above the free surface of the water tanks. At this time, a vacuum is created at the top of the system. This is done by controlling the seawater intake valve B located in the seawater tank below the evaporator column. When the evaporation column is heated (by any energy source) while

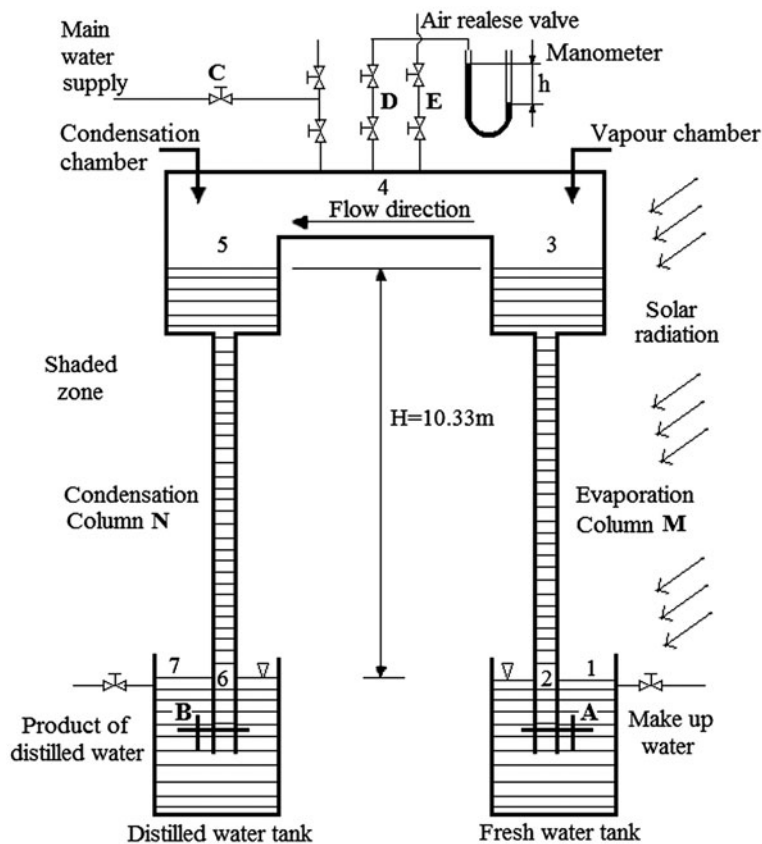


Fig. 1. Theoretical model of the NVDU.

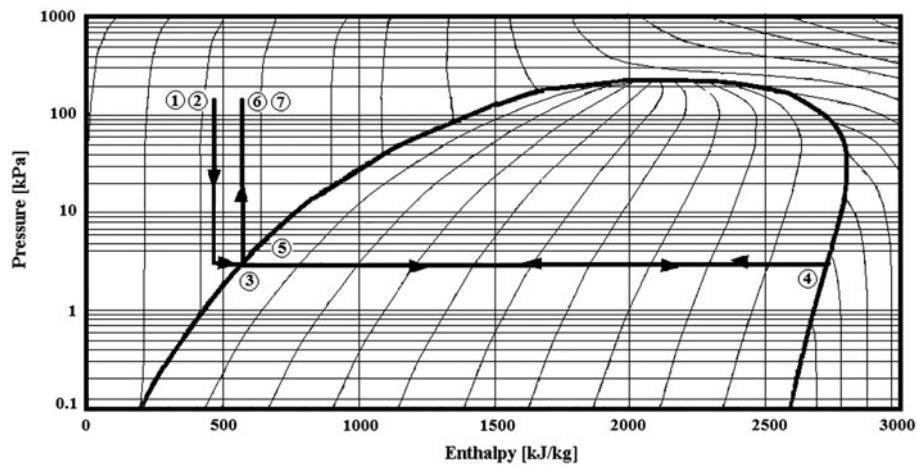


Fig. 2. The thermodynamic cycle of the operation process.

the condensation column is cooled (naturally in the atmospheric air or using a cold sink), the temperature difference at the top of these columns drives the water vapor continuously in the vacuum chamber, where the pressure is below atmospheric pressure.

To simulate the system performance, mass, energy, and salt balance were obtained using the equations suggested by Alezzi and Ayhan [10] with the same assumptions as in their study, as follows:

- (1) The connecting pipe wall between the saline and freshwater chambers is adiabatic (no heat is transferred from or to the vapor traveling between the two chambers; hence, the temperature of the vapor does not change before it reaches the freshwater chamber).
- (2) Noncondensable gases released from saline and freshwater masses have no effect on the vapor pressure inside the system.
- (3) The corners of the pipe connecting the two chambers do not affect the pressure of the vapor traveling from the saline to the freshwater chamber.

3. Experimental setup

The experimental setup is schematically illustrated in Fig. 3. The NVDU consisted of two parts, a top part and a bottom part. The evaporation and condensation chambers, feed tank, vacuum pump, and chiller unit were placed in the top part of the system, while the balance columns were situated in the bottom part. The evaporation and condensation chambers were connected by a steel pipe of 250 mm diameter and 5 mm thickness. The surfaces of the condensation chamber and the connecting pipe surface were cooled by means

of a coil wound round their outer surfaces and covered by insulating material to avoid heat gain from the surroundings. An auxiliary electrical heater was placed inside the evaporation chamber to heat the water at night, and the seawater inlet was heated by an external auxiliary heater during the day. Four mercury manometers and pressure sensors were connected to the surface of the connecting pipe to indicate the operating pressure and/or pressure loss in the system. The condensation chamber, which is one of the most important components of the system, was cooled by a water jacket-type heat exchanger. Water levels in both chambers were observed using water level indicators. The feed tank for the vacuum pump was made of steel of 5 mm thickness with a closed volume of $0.5 \times 0.7 \times 0.5 \text{ m}^3$ and used to keep the natural vacuum of the system in case of insufficient production of freshwater during distillation. A water-ring vacuum pump, 1.6 kW, was connected to the system to compensate pressure losses during the experiments.

The water-ring vacuum pump, connected to the NVDU and the direct condensation tank, is shown in Fig. 4. The balance column of the evaporation tank was made of 50 mm copper pipe and the balance column of the condensation tank was made of 50 mm PVC pipe.

Transparent pipe of 50 mm diameter was used to monitor freshwater production. This was placed in the bottom part of the experimental setup.

Firstly, the filling and leakage points in the NVDU were controlled to prevent involuntary losses during the experiments. This was done by filling the system with water while the operation valves were closed and the system was pressurized. In order to create a natural vacuum in the system, valves A and B were

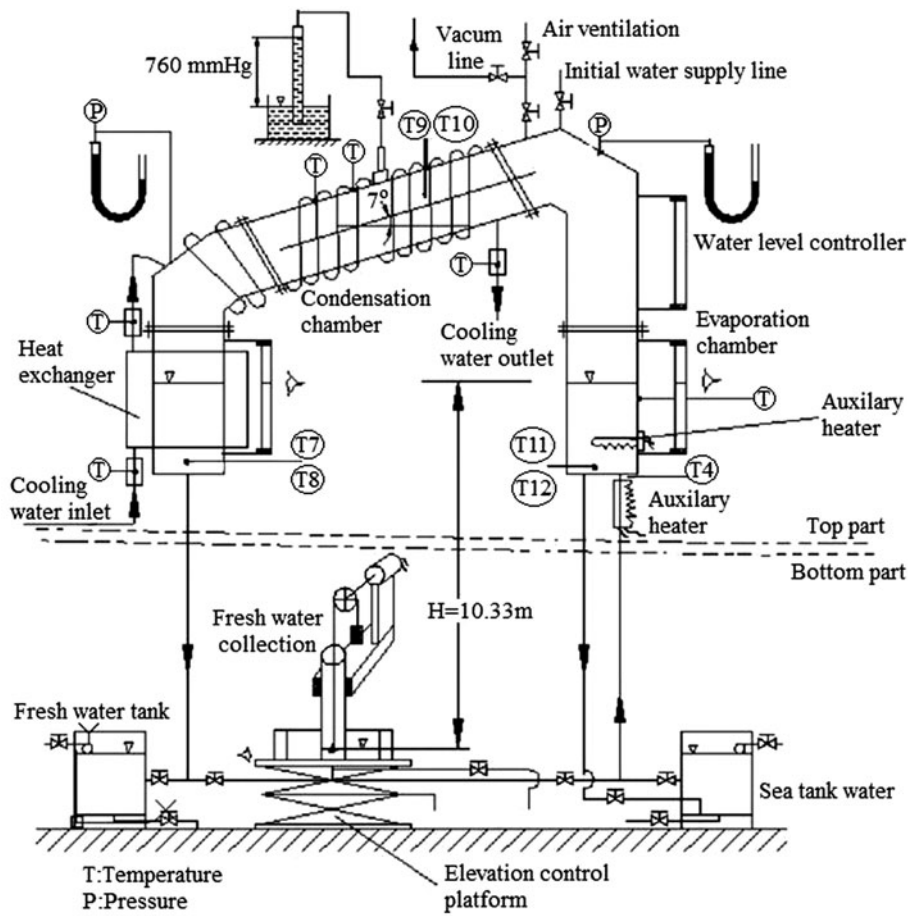


Fig. 3. Schematic illustration of the experimental setup. T4: seawater supply temperature in °C; T7 and T8: freshwater temperature in the condenser in °C; T9 and T10: transport steam temperature in °C; and T11 and T12: seawater temperature in the evaporator in °C.

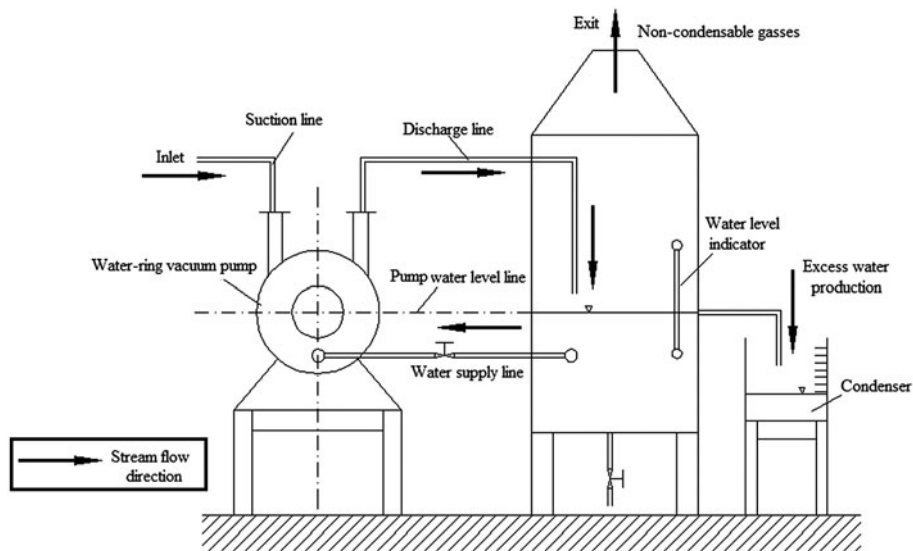


Fig. 4. Water-ring vacuum pump and direct condensation process.

opened while the freshwater level in the transparent freshwater collection pipe was observed. The process flowchart of the NVDU is shown in Fig. 5.

The vapor produced in the evaporation chamber was transferred to the condensation water tank by means of mass convection. The vapor condensed in the condensation chamber. The freshwater accumulating in the condensation chamber was removed through the condensed water balance column. When the level of water in the system fell during the experiments, the vacuum pump was used to keep the manometric height constant at 10.33 m of water in the system.

Using this experimental apparatus, the NVDU was tested under three sets of conditions or operating modes, in the outdoor conditions of Bahrain.

3.1. First operating mode (low velocity evaporation)

The first operating mode was similar to the design shown in Fig. 3 without a water-ring vacuum pump.

The conditions were set such that the temperature of the condensation chamber was kept constant at around 25°C using the main water supply. Direct solar energy was used as a heat source for the evaporation chamber. Phase change (evaporation) took place under the thermodynamic equilibrium state, as the vapor velocity was very low.

3.2. Second operating mode

The second mode involved the boiling of seawater, so that the fluid flow would enhance the effects of cavitation.

Under this second set of operating conditions, unstable buoyancy-induced fluid flow was established through the supply of seawater to the NVDU. In order

to create buoyancy-driven flow, the seawater temperature was kept higher than the evaporation temperature. The supplied seawater was heated by an auxiliary electrical heater. During the experimental studies, a water-ring vacuum pump was used to compensate the pressure drops in the system. The periodic operation of the pump also caused the fluid flow to become pulsating in nature. During the experiments, condensation was achieved by convective cooling to the ambient air, while evaporator temperatures were fixed at 45, 50, and 55°C using an auxiliary electrical heater, and the seawater supply temperature was kept at 65°C. Design of the buoyancy-induced cavitating flow is shown schematically in Fig. 6.

3.3. Third operating mode

Under the third set of operating conditions, the cooling water temperature for the condensation process was kept constant at 12°C using chilled water, while evaporator temperatures were fixed at 45, 50, and 55°C using an auxiliary electrical heater.

During the experimental studies, a water-ring vacuum pump was used to compensate the pressure drops in the system. The temperature difference between the evaporation chamber and condensation chamber increased the pressure difference, as a result of which the vapor molecules moved faster than under the first operating mode, causing a decrease in pressure at the interface of liquid water in the evaporation chamber and water bubbles generated due to evaporation. On the other hand, decreasing the pressure caused cavitation in the liquid phase. Contributions of the water-ring vacuum pump were also noticeable in discharging noncondensable gases and compensating pressure losses periodically. The

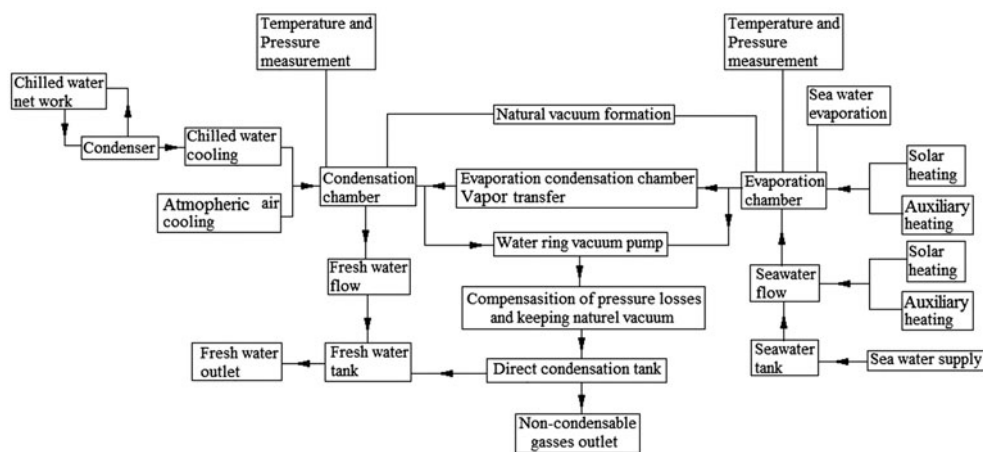


Fig. 5. Process flowchart of NVDU.

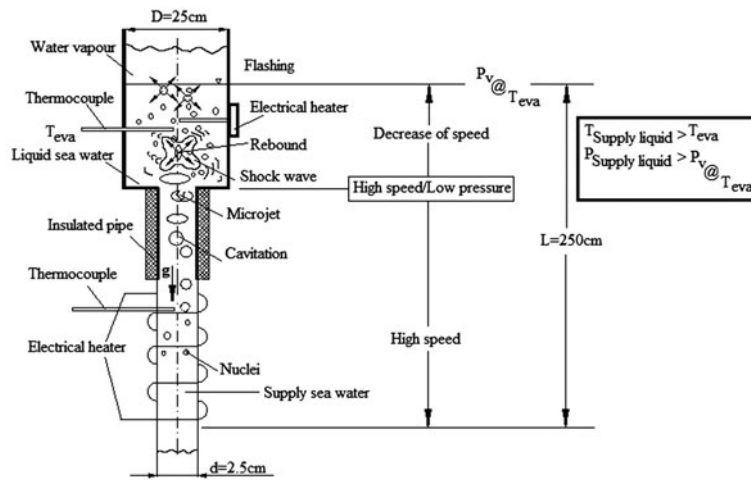


Fig. 6. Schematic presentation of buoyancy-induced cavitating fluid flow in the NVDU.

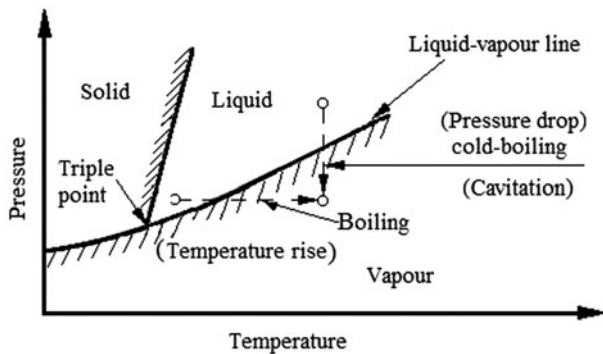


Fig. 7. Hot and cold boiling (cavitation).

two processes are shown in the sketch of a P - T diagram in Fig. 7.

A typical sudden enlargement of the flow domain was noticed where the evaporation chamber and seawater supply pipe were connected. The flow field promoted the mixing and collapse of cavitation bubbles and produced noise [11,12]. These effects were observed at the interface of the vapor and liquid phases, and contributed to flashing at the interface surface. Because of the balance of two competing mass fluxes driven by buoyancy and evaporation, the evaporation rate in the evaporation chamber increased dramatically and this was observed experimentally.

4. Instrumentation

During the NVDU experiment, time, pressure, temperature, energy, water level in the columns, solar intensity and the amounts of freshwater were mea-

sured with the appropriate instruments. All instrumentation devices were calibrated before use.

5. Uncertainty analysis of the data

Uncertainty in the experimental data is considered by identifying the main sources of error in the primary measurements, such as time, water level, electrical energy, voltage, current, pressure, and temperature. The uncertainty in time measurements was ± 0.01 s. The power supplied to the heaters in the evaporator column and seawater tank was determined by monitoring the applied voltage and current with an accuracy of 1%. Thus, the uncertainty in the heat input rates was calculated as 1.4%. The heights of the liquid columns were manually read by sight using distance markers, whose thickness causes an uncertainty of ± 0.5 mm in the column height readings. The effective vapor pressure was measured by a Validyne

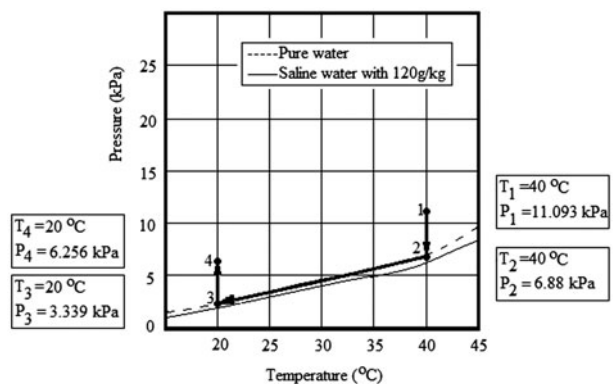


Fig. 8. Typical data for the test.

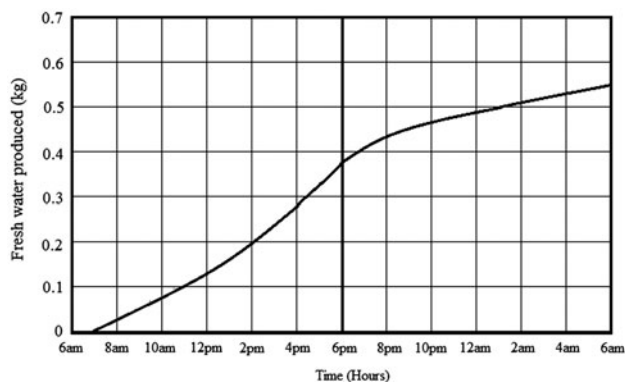


Fig. 9. Freshwater produced for hot weather in Bahrain.

differential pressure transducer with an accuracy of 0.25% together with U-tube mercury manometers with an uncertainty of 0.5 mm Hg. The temperatures were measured by a computer-controlled data acquisition system with an accuracy of $\pm 0.5^\circ\text{C}$. The solar intensity was measured by a Kimo-SL 100 Solarimeter. Limiting error propagation on the mass production rate was found to be ± 0.5 kg/s.

6. Results and discussion

6.1. First operating mode

Typical results under the first set of operating conditions are presented in Figs. 8 and 9.

These results verify those for the first set of operating conditions studied by Alezzi and Ayhan [10].

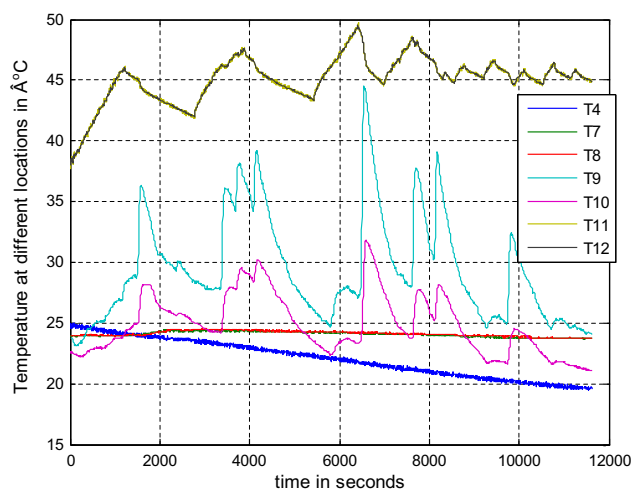


Fig. 10. Temperature variation at different locations against time (7 March 2013, from 5.30 to 7.30 pm in Bahrain. Absolute vacuum was 9.6 ± 0.5 kPa and average environmental temperature was $18 \pm 0.5^\circ\text{C}$).

Their results for the mathematical model of the NVDU are presented in Figs. 8 and 9.

The values for freshwater produced, shown in Fig. 9, are based on two assumptions: that all vapor produced is condensed in the freshwater chamber, and that the effect of noncondensable gases is negligible. According to the calculations of Alezzi and Ayhan, 0.54 kg of freshwater is produced in 24 h [10]. Approximately 67% of this is produced during daylight hours and the rest at night, when no heat is supplied and the saline water evaporates by utilizing stored energy. As the saline water continues to produce vapor, the stored energy is carried away as latent heat, thus reducing the temperature until evaporation eventually stops.

6.2. Second operating mode

In order to investigate the effects of buoyancy-driven flow and cavitation on the performance of the system, the operating conditions of the vacuum pump were controlled, while seawater supply temperature was kept higher than evaporation temperature in the evaporation chamber.

6.2.1. Tests in the absence of buoyancy forces

Typical results of the variation in the vacuum pressure and vapor temperature in the vacuum chamber, evaporation and condensation temperatures, and ambient temperature during the hours of the experiment are shown in Fig. 10, where temperatures T9

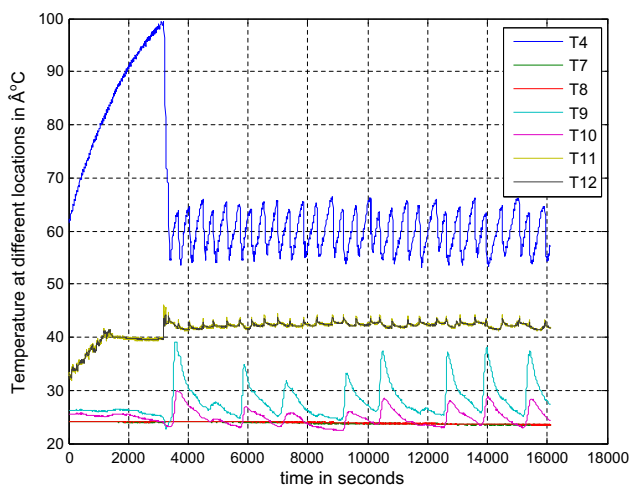


Fig. 11. Temperature variation at different locations against time (21 March 2013, from 5.30 to 7.30 pm in Bahrain. Average absolute vacuum was 9.2 ± 0.5 kPa and average environmental temperature was $24 \pm 0.5^\circ\text{C}$).

and T10 indicate the behavior of the water-ring vacuum pump.

The effect of the removal of noncondensable gases can be attributed to variation in the evaporation temperature due to the creation of a vacuum at the evaporation surface. During the suction phase of the water-ring pump, seawater entered the evaporation chamber until the setup temperature was reached; then, the pump stopped and the evaporation process continued until the next suction phase started. The auxiliary heater compensated the energy required for evaporation at set temperature and pressure. The flow of seawater through the evaporation chamber was pulsative in nature. On the other hand, use of the auxiliary heater caused surface temperature cavitation to occur. Cooling was achieved by convection heat transfer from the condenser surface to the ambient air. The combined effect was an increase in evaporation rate. The overall accumulated freshwater production rate was measured at 0.30 kg/h, which is 14 times greater than under the first set of operating conditions.

6.2.2. Tests in the presence of buoyancy forces

Under these operating conditions, the researchers studied the effects on the freshwater production rate of buoyancy forces created by the difference between seawater temperature (T4) and evaporation temperature (T11 and T12). Typical results for the operation period of the vacuum pump can be seen in Fig. 11, which also shows vapor temperature in the vacuum

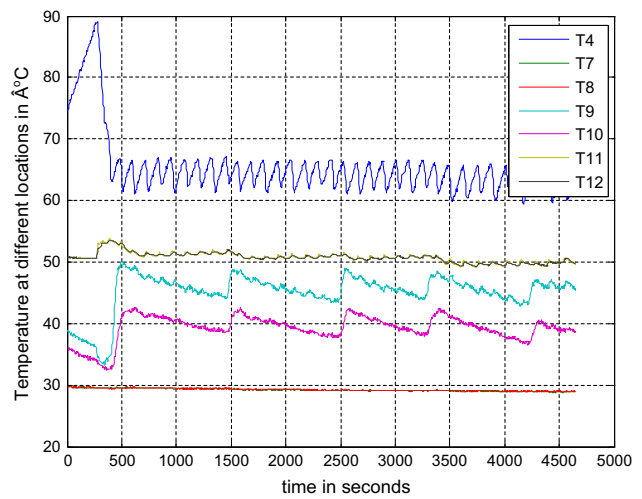


Fig. 13. Temperature variation at different locations against time (6 April 2013, from 16.15 to 17.35 pm in Bahrain. Average absolute vacuum was 12.4 ± 0.5 kPa and average environmental temperature was $24 \pm 0.5^\circ\text{C}$).

chamber, evaporation and condensation temperatures (T7 and T8), and ambient temperature during representative times of testing. The overall accumulated freshwater production rate was measured at 0.37 kg/h, i.e. fifteen times greater than under the first set of operating conditions. The temperature variations in Figs. 11–13 show the combined effects on the freshwater production rate of buoyancy forces and the removal of noncondensable gas.

It is obvious that the pump operation period during the process in Fig. 12 was longer than that in

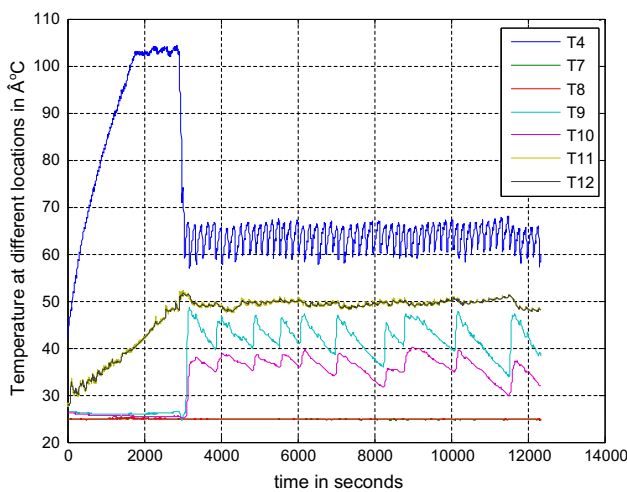


Fig. 12. Temperature variation at different locations against time (23 March 2013, from 3.50 to 7.00 pm in Bahrain. Average absolute vacuum was 10.9 ± 0.5 kPa and average environmental temperature was $24 \pm 0.5^\circ\text{C}$).

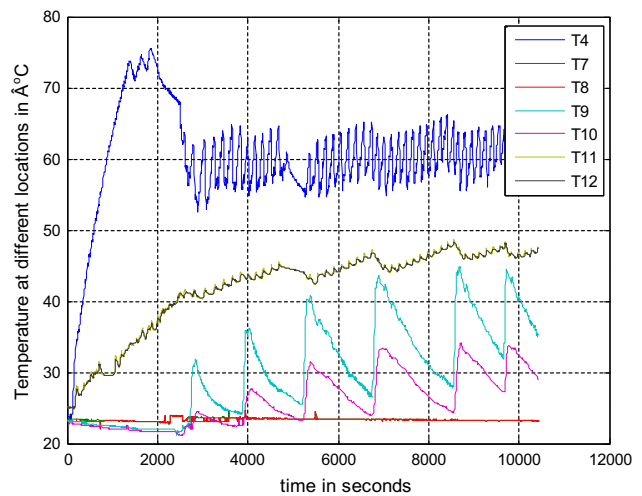


Fig. 14. Temperature variation at different locations against time (25 March 2013, from 18.00 to 20.00 pm in Bahrain. Average absolute vacuum was 7.0 ± 0.5 kPa and average environmental temperature was $19.5 \pm 0.5^\circ\text{C}$).

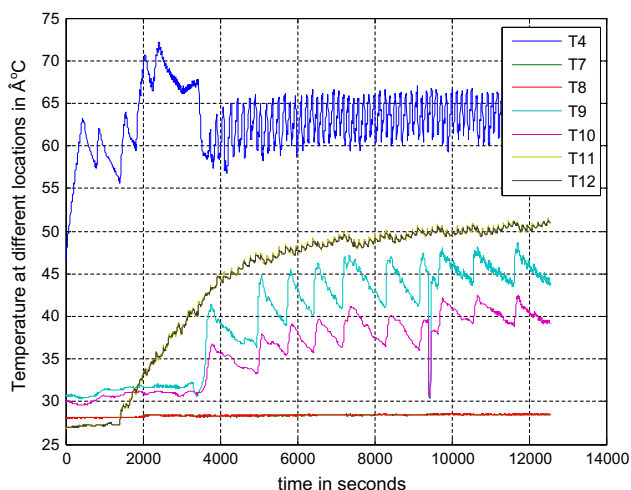


Fig. 15. Temperature variation at different locations against time (6 April 2013, from 13.00 to 14.45 pm in Bahrain. Average absolute vacuum was 9.8 ± 0.5 kPa and average environmental temperature was 26.5 ± 0.5 °C).

Fig. 11. The overall accumulated freshwater production rate was measured at 0.40 kg/h, eighteen times greater than under the first set of operating conditions. Similar results are shown in Fig. 13 for a longer period

of time, where the freshwater production rate was again about 0.40 kg/h. The cost of freshwater is calculated as 2.5×10^{-3} BD/kg, based on electricity consumption for the water-ring vacuum pump and the cost of power generation in Bahrain. In order to clarify the transient period of the processes, typical experimental results are presented in Figs. 14 and 15. The freshwater production rate in the transient period was found to be about 2–6% of the accumulated freshwater production in the processes.

6.2.3. Third operating mode

Under the third set of operating conditions, the temperature of the cooling water for the condensation process was kept constant at 12 °C using chilled water, while evaporator temperatures were fixed at 40, 50, and 60 °C using the auxiliary electrical heater, and the vacuum pressure was controlled by the water-ring vacuum pump. Cavitated flow was generated as a result of unstable boiling on the surface of the heater. The periodic operation of the water-ring vacuum pump helped to remove noncondensable gases from the system, which enhanced the freshwater production rate. The comparison of the enhanced freshwater

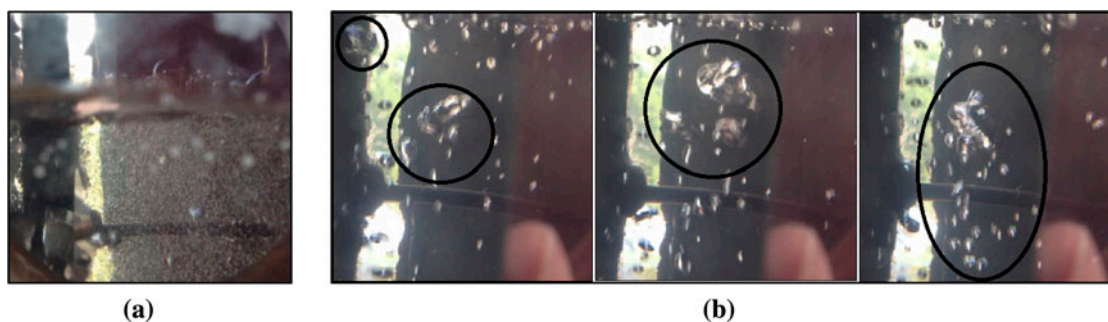


Fig. 16. Visualization of bubble dynamics (a) and merging and coalescence phenomena (b). (The vessel temperature was 34.6 °C and the ambient temperature was 16.1 °C. The vacuum pressure was measured at 13.33 kPa (absolute).)

Table 1
Experimental results

No. of run	Pressure (kPa)	Evaporation temperature (°C)	Amount of freshwater (L/h)	Percentage increase
1	10.64	50	0.436	1,453
2	10.64	60	1.626	5,420
3	9.31	40	0.166	553
4	9.31	50	0.88	2,933
5	9.31	60	1.93	6,433
6	7.98	40	0.374	1,246
7	7.98	50	1.112	3,706
8	7.98	60	2.10	7,000



Fig. 17. Visualization of water surface flashing in the vessel. (The vessel temperature was 34.6 °C and the ambient temperature was 16.1 °C. The vacuum pressure was measured at 13.33 kPa (absolute).)

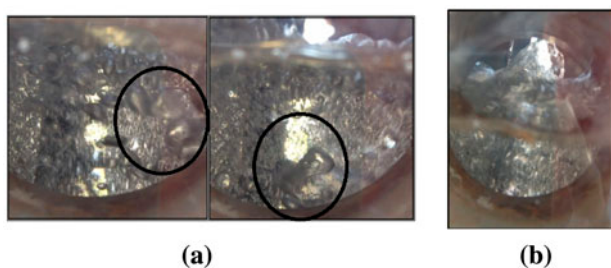


Fig. 18. Visualization of bubble merging and coalescence in bubble motion phenomena (a) and surface flashing (b). (The vessel temperature was 55.6°C and the ambient temperature was 17.2°C. The vacuum pressure was measured at 51.0 kPa (absolute).)

production rate was made on the basis of the first operating mode (0.030 L/h). This mode of NVDU operation is suitable for wastewater treatment in cold climates. Typical experimental results are presented in Table 1 for the nonequilibrium conditions.

6.2.4. Visualization of bubble motions

In order to verify the experimental results, a new dummy experimental setup was designed having similar geometry to the prototype and manufactured for the visualization of bubbles motions. The system was operated under conditions similar to the third operating mode. The bubble motions in the combined cold and hot cavitations and their effects on flow phenomena were observed. Some typical results are shown in Figs. 16–18.

7. Conclusion

This study extends the work of Alezzi and Ayhan [10], who examined the thermodynamic feasibility of NVD in Bahrain. The new contribution herein is the

extension to the enhancement of freshwater production rates. A significant new result, not reported in previous work, is that the freshwater production rates increase under operating conditions where cold and hot boiling occur together in the evaporation chamber. This operating mode increases evaporation rates, while modification of the condenser temperature affects the cost of freshwater production in Bahrain.

The study suggests that operating conditions be designed such that hot evaporation is created by means of buoyancy forces and cold evaporation is created by means of the natural vacuum technique with the aid of a water-ring vacuum pump.

Apparently, the physical phenomenon of the combined effects of the cold and hot boiling evaporation applied to the NVD system in Bahrain was observed for the first time.

Freshwater production rates increased eighteen times as compared to the conventional operational methods of the NVD systems in Bahrain. Freshwater production cost could be reduced to approximately 2.5×10^{-3} BD/kg h from a cross-sectional surface area of 0.0490 m² for the evaporation chamber.

The application of a combined hot and cold boiling operating mode for the NVDU appears to be the most promising technique for wastewater treatment using waste heat or energy in cold climatic zones.

Acknowledgments

This work was supported by the University Bahrain Deanship of Research under Grant (2008-10).

Devices were fabricated in the Mechanical Engineering Workshop at the University of Bahrain.

References

- [1] G.F. Leitner, Is there a water crisis? *Int. Desalin. Water Reuse Q.* 7(4) (1998) 10–21.
- [2] M. Al-Rashed, M. Sherif, Water resources in the GCC countries: An overview, *Water Resour. Manage.* 14 (2000) 59–75.
- [3] Khater, Water Situation in Bahrain, s.l., Internal Report, 1999.
- [4] G. Bemporad, Basic hydrodynamic aspects of a solar energy based desalination process, *Solar Energy* 54 (1995) 125–134.
- [5] A. Midilli, T. Ayhan, Natural vacuum distillation technique—Part I: Theory and basics, *Int. J. Energy Res.* 28 (2004) 355–371.
- [6] A. Midilli, T. Ayhan, Natural vacuum distillation technique—Part II: Experimental investigation, *Int. J. Energy Res.* 28 (2004) 373–389.
- [7] H. Al-Madani, T. Ayhan, Feasibility study of renewable energy powered seawater desalination technology using natural vacuum technique, *Renew. Energy: Int. J.* 35(2) (2010) 506–514.

- [8] G. Veeragnaneswar, N. Nermalakhandan, Desalination using low grade thermal energy, s.l., in: Third International Conference on Thermal Engineering Applications and Theory, Amman, 2007.
- [9] H. Al Madani, T. Ayhan, Feasibility study of renewable energy powered natural vacuum technique for seawater desalination, in: Seventh Conference on Sustainable Development of Energy, Water and Environment Systems, Orhid, Macedonia, 2012.
- [10] Y. Alezzi, T. Ayhan, Natural Vacuum Desalination performance in Bahrain: Theoretical Study, in: Second International Science and Technology Conference, Dubai, 2012.
- [11] J.R. Blake, D.C. Gibson, Growth and collapse of a vapour cavity near a free surface, *J. Fluid Mech.* 111 (1981) 123–140.
- [12] C.E. Brenne, *Cavitation and Bubble Dynamics*, Oxford University Press, New York, NY, 1995.